



## Antibacterial Assessment of Biofabricated Magnesium Oxide Nanoparticles (MgO NPs) using *Conocarpus erectus* Leaf Extract

Shahid Ullah Khan<sup>1</sup>, Umber Zaman<sup>2</sup>, Khalil ur Rehman<sup>2\*</sup>, Uzma Faryal<sup>1</sup>, Dilfaraz Khan<sup>2</sup>, Sumbul Saeed<sup>3</sup>, Madeeha Jadoon<sup>1</sup>, Muhammad Hafeez Ullah Khan<sup>3</sup>, Muneeb Ullah<sup>4</sup>, Aneela Bashir<sup>5</sup>, Masooma Rafique<sup>6</sup>, Wasim Ullah Khan<sup>7</sup>, Qazi Shoaib Ali<sup>8</sup>, Muhammad Asif Ismail<sup>9</sup>, Bibi Hajira<sup>1</sup>, Ayesha Asad<sup>10</sup>

<sup>1</sup>Department of Biochemistry, Women Medical and Dental College, Khyber Medical University KPK, Pakistan.

<sup>2</sup>Institute of Chemical Sciences, Gomal University, Dera Ismail Khan 29050, Pakistan.

<sup>3</sup>National Key Laboratory of Crops Genetics and Improvement P. R. China.

<sup>4</sup>Department of Pharmacy, Kohat University of Science and Technology, Kohat, Khyber Pakhtunkhwa, Pakistan.

<sup>5</sup>Department of Soil Sciences, Faculty of Agriculture, Gomal University, Dera Ismail Khan 29050, Pakistan.

<sup>6</sup>Department of Medical Education, Women Medical & Dental College, Abbottabad.

<sup>7</sup>State Key Laboratory of Optoelectronic Materials and Technologies, School of Materials Science and Engineering, Sun Yat-sen University, Guangzhou 510275, PR China

<sup>8</sup>Department of Horticulture, The University of Agriculture Peshawar Pakistan

<sup>9</sup>College of food science and technology, Huazhong agricultural university, 430070, Wuhan P.R. China, Functional food engineering and technology research Centre of Hubei province.

<sup>10</sup>Army Medical College, Rawalpindi

### Abstract

Nanobiotechnology is an advanced discipline of science that deals with nanoscale materials in areas including nanotechnology, chemistry, medicine, and biotechnology. The current trend is to use sustainable and biological methods utilizing natural sources to quickly synthesize metal oxide nanoparticles rather than toxic, dangerous biochemical ones. In this paper, the biogenesis of magnesium oxide nanoparticles (MgO NPs) utilizing *Conocarpus erectus* as a natural source is described for the first time. In producing MgO NPs, *C. erectus* leaf extract was a bioreductor and stabilising agent. Several characterisation techniques, including XRD, FTIR, HRTEM, SEM, and EDX studies, were employed to confirm the formation, crystalline structure, and surface morphology of the synthesized nanoparticles. XRD measurement confirmed the crystalline f.c.c structure of MgO NPs. The production and stabilisation of MgO NPs by *C. erectus* leaf extract were attributed by FTIR analysis to the active functional groups. Studies using HRTEM and SEM revealed that the magnesium oxide nanoparticles were small-sized, spherical, and uniformly dispersed. The EDX profile also approved the elemental composition of the produced nanoparticles. The bacterial inhibition by the synthesized MgO NPs was evaluated against *S. aureus* and *E. coli* that plant-mediated MgO NPs effectively inhibited, with inhibition zones of 17(±0.4) mm and 16(±0.5) mm, respectively.

**Keywords** Biofabrication, *Conocarpus erectus*, MgO NPs, Antibacterial activity

## 1. Introduction

Nanotechnology is a sponsoring area of material science that is proficient in fabricating nano-scale materials. A broad category of materials known as "nanomaterials" consists of particles with sizes between 1-100 nm (1). Nanotechnology has broadly produced efficient catalysts that are biochemically active in regulating various infections caused by pathogenic microbes. In current eras, metal and metal oxide NPs have attained much more interest among

researchers due to their infrequent possessions as opposed to other nanoparticles (2). MONPs have extensive biological and therapeutic applications as alternate anti-microbial mediators ascribed to the reoccurrence of contagious infections and the arrival of antibiotic-resistant strains. MgO NPs have been used in contaminated waste remediation, antiseptic, electronics, paints, optical, antibacterial agents, semiconductors, catalysis, and catalytic devices (3-11).

**Corresponding author at:** Khalil ur Rehman  
**Email address:** [rehmankhalil025@gmail.com](mailto:rehmankhalil025@gmail.com)

<https://doi.org/10.56600/jwmdc.v1i2.21>

Typically, the photodegradation of MB dye and bacterial obstruction is accomplished in the attendance of MONPs, which impede the growth of bacteria and deprive toxic dye by generating reactive oxygen species (ROS) (12, 13).

Generally, metal and MONPs have been fabricated using conventional chemical and physical procedures that are toxic, costly, and cause several ecological and health problems (14, 15). The preparation of metal and MONPs using plant extract is an appealing approach compared to other routes (16-21). The biochemical preparation of MONPs by plant arbitrated route has the aid of being facile, innocuous, and biodegradable (22-24). Phytochemicals of plant sources performed an imperative role in the development and stabilization of nanomaterials. Accordingly, assets of the created NPs, i.e., antibacterial activity and biocompatibility based on the possessions of biomolecules of the plant source from which they were prepared. Several reports have been available regarding the fabrication of MgO NPs via green synthetic procedures. Several plant extracts, i.e., white button mushroom (25), *Rosmarinus officinalis* (26), *Trigonella foenum-graceum* (27), *Embllica officinalis* (28), *Trigonella foenum-graecum* (29), *Matricaria chamomilla* (30), etc., were reported for the green synthesis of MgO NPs. In this study, MgO NPs were biochemically prepared using leaf extract of *C. erectus*. The mangrove shrub *C. erectus*, also referred to as green buttonwood or button mangrove, belongs to the *Combretaceae* family (31), cultivated on coastlines in sultry and sub-tropical areas of the biosphere (32). This plant is also widely grown as ornamental furniture, for land reclamation, as a hedge, and as a very hard and strong wood (33). This plant species has been used traditionally by local people for the treatment of various such as headache, anemia, orchitis, bleedings, prickly heat, diabetes, catarrh, syphilis, gonorrhoea, tumors, conjunctivitis, swellings, antipyretic and anti-inflammatory, etc. (34-37). *C. erectus* has shown strong antioxidant, antibacterial, anticancer, hepatoprotective, DPPH assay, and antimicrobial activities (38-41). A number of phytochemicals, such as gallic acid, tannins, phenolics, terpenoids, flavonoids, etc., were found in the leaf extract of *C. erectus* (42-43). Due to such phyto constituents, *C. erectus* intensely played a crucial role in developing magnesium oxide NPs.

Thus in this report, we have successfully synthesized MgO nanoparticles by an eco-friendly, nontoxic, green deposition method using *C. erectus* leaf extract as stabilizing and reducing mediator. Additionally, MgO NPs were tested for the inhibition of bacteria. The naturally accessible and harmless plant source was used to manufacture MgO NPs.

## 2. Experimental

### 2.1 Materials

Magnesium sulphate heptahydrate ( $\text{MgSO}_4 \cdot 7\text{H}_2\text{O}$ ), methylene blue, sodium hydroxide, nutrient agar, nutrient broth, and all other chemicals used in this report were procured from Sigma Aldrich (Pakistan). All the chemicals and reagents were of optimal purity and used without further sanitization.

### 2.2 Leaf Extract Preparation

Fresh and unspoiled leaves of *C. erectus* were calm from D. I. Khan, KPK, Pakistan. The leaves were eroded with deionized water, allowed to desiccate at room temperature, and then mechanically ground into powder. 5g leaf powder was added to 120 mL of water, and mixture was agitated for 5 hrs at 40 °C (see Figure 1A). Finally, the supernatant was filtered and kept at 4 °C.

### 2.3 Biosynthesis of MgO NPs

To synthesize MgO NPs, 1.2 g  $\text{MgSO}_4 \cdot 7\text{H}_2\text{O}$  (0.1 M) was added to 100 mL of water. The mixture was agitated at 70 °C for 3 hrs to form a homogeneous solution. NaOH (1M) solution was added dropwise with the help of a burette, and the mixture was stirred again for the next 1 hr. Green extract of *C. erectus* was added drop wise at continuous stirring. The appearance of brown color confirms the creation of MgO nanoparticles, as illustrated in Figure 1(B). The color change prompted the reduction of Mg to MgO NPs. The solution was centrifuged (3500 rpm, 10 mints), and the precipitates were cleansed with acetone and then deionized water to eradicate the unwanted impurities. The nanoparticles were dried for 12 hrs at 80 °C in an electric oven. Finally, after being calcined for three hours at 400 °C in a Muffle furnace, the well-dried MgO NPs were produced as pale yellow MgO nanoparticles.

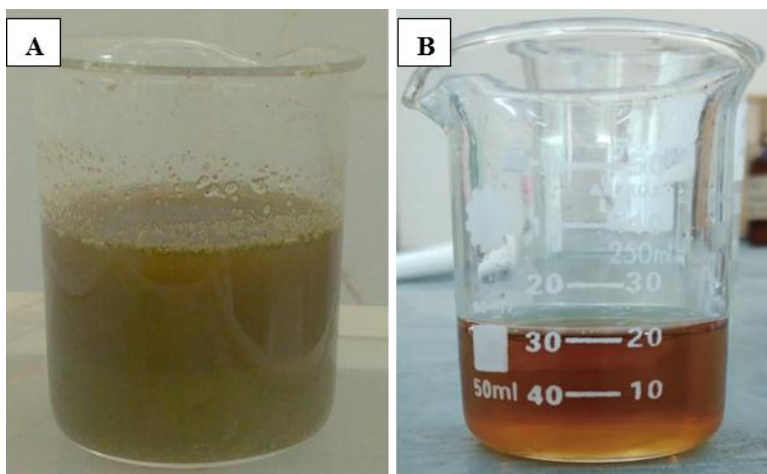


**Figure 1:** (A) Leaf extract and (B) MgO NPs

#### 2.4 Antibacterial Assessment of MgO Nanoparticles

The antibacterial activity of biogenic MgO nanoparticles was tested by using *S. aureus* and *E. coli* bacteria. These strains were obtained from the Department of Biotechnology, Gomal University, Dera Ismail Khan. These strains were kept on agar slants at 4 °C for the antibacterial assay. The bacteria were incubated for 24 hrs at 37 °C in Muller Hinton Broth (Oxoid) with a pH of 7.2. An agar well diffusion procedure was applied to scrutinize the antibacterial assessment of biosynthesized magnesium oxide nanoparticles (44). The bacterial strains were cultured in nutrient broth for 24 hrs at 37 °C in an incubator. To ensure a consistent, dense sheet of growth after incubation, the inocula of the specific bacteria were patterned onto the Muller Hinton agar platters using a sterile swab. Boreers (6 mm) were designed using disinfected cork bradawl onto the nutrient agar plates. In the agar, well diffusion method, 1mg MgO NPs was added with 1 mL of deionized water. The sterile bores were soaked with 50 mL of MgO nanoparticles with a high concentration of respective agar bioassay. The MgO NPs integrated wells were sited onto petri dishes and incubated at 37 °C for 24 hrs. The embarrassment regions were measured very cautiously.

##### 2.4.1 Determination of MIC

MIC is the least quantity of material that stop bacteria from growing. The MIC of biodirectedMgO NPs can be examined by serial dilution strategy. Different concentrations of greener MgO NPs were treated with 1 mL of bacterial solution. The suspension turbidity was adjusted to 0.5 McFarland turbidity standards. 1 mgmL<sup>-1</sup> to 0.125 mgmL<sup>-1</sup>

concentration of biomediated MgO NPs were added to the test tubes. These test tubes were then kept at 37 °C for an overnight incubation period. The control was a test tube containing growth media and a bacterial solution. The assay was repeated thrice.

#### 2.5 Characterization

The wide angle XRD pattern of MgO NPs was recorded by using Rigaku D/Max2500 VBZ+/PC Diffractometer. An ABB MB 3000 Spectrophotometer was applied for recording FTIR spectra of plant extract and biosynthesized MgO NPs. The size and dispersion of MgO NPs were analyzed using HRTEM (JEM-3010 Microscope). The surface morphology and elemental composition of the sample material were examined using a Hitachi S-4700 SEM.

### 3. Results and Discussions

#### 3.1 XRD Analysis

Structural exploration of greener magnesium oxide NPs was done using an X-ray diffractometer. Figure 2 symbolizes the characteristic XRD pattern of biodirected magnesium oxide NPs. The angle (2θ) range was adjusted between 30-80°. The result shows that five well-observed peaks have appeared 38.34°, 44.58°, 65.35°, 74.6° and 79.3° which can be indexed to (111), (200), (220), (311), and (222) Bragg reflections of the f.c.c structure of MgO NPs. The result matched with JCPDS-21-1272. The most prominent peak at 38.34° (111) can be attributed to the f.c.c crystal structure of MgO NPs the results matched the previously reported work (45). The diffractogram exhibits no ancillary phase or impurity peaks.

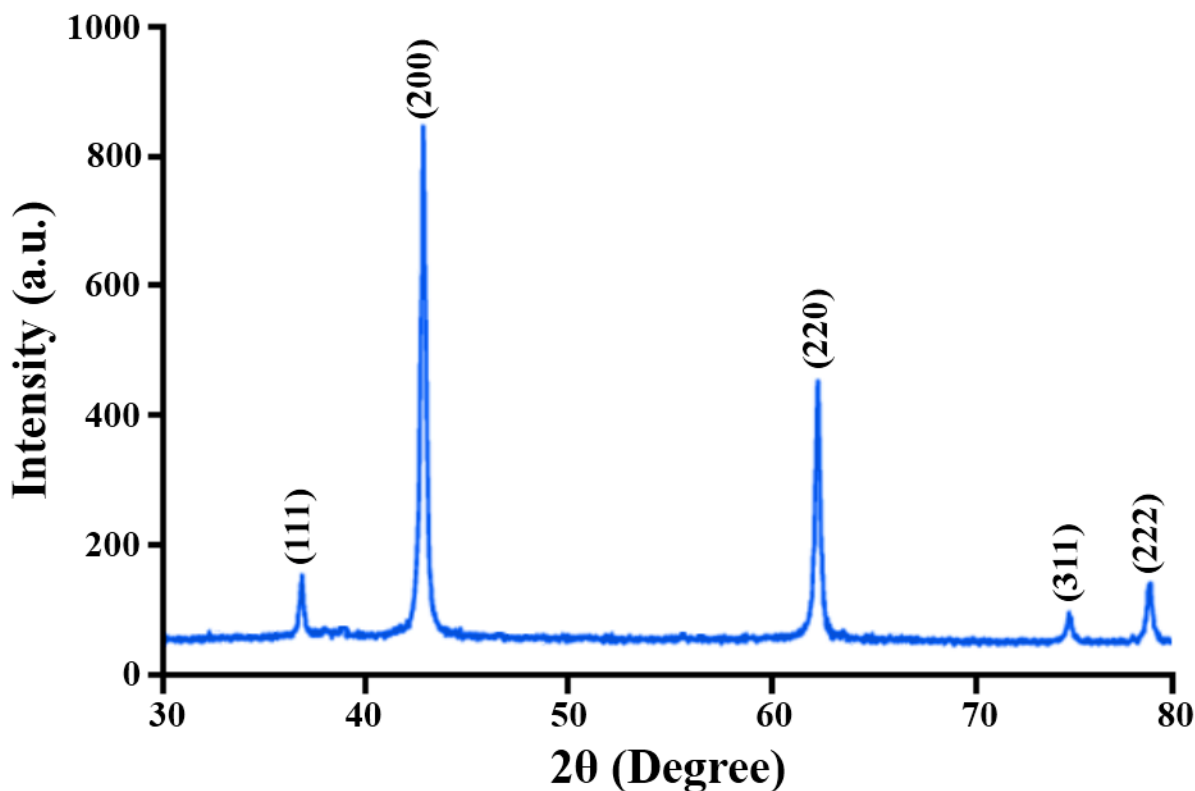


**Figure 2:** XRD pattern of biosynthesized MgO NPs

### 3.2 FT-IR Spectral Analysis

FT-IR study was performed to specify the phyto constituents of *C. erectus* liable for the formation and stabilization of MgO NPs. FT-IR spectra of leaf extract and biomediated MgO NPs are illustrated in Figure 3. The results confirmed that the plant precursors act as stabilizing and reducing mediators. The major peaks at  $3332\text{ cm}^{-1}$  confirm the stretching vibrations of O—H bonds, which confirm the phenolic character of plant extract. The peaks at  $2932\text{ cm}^{-1}$  are associated with the C—H stretching vibrations by

confirming the aldehydic character of plant extract. The bands at  $1613.4\text{ cm}^{-1}$  reflect the C=C stretching frequencies, whereas the arrival of the bands at  $1500\text{ cm}^{-1}$  are due to N—N bending vibrations. The peaks at  $1064.48\text{ cm}^{-1}$  are related to the bending frequencies of absorbed water molecules and surface O—H radicals. A well-observed peak at  $534.7\text{ cm}^{-1}$  indicates a C—O diagnostic bond confirmed the development of MgO NPs. The results clear that most of the biomolecules found in plant extract were intricate in the formation of NPs (46).

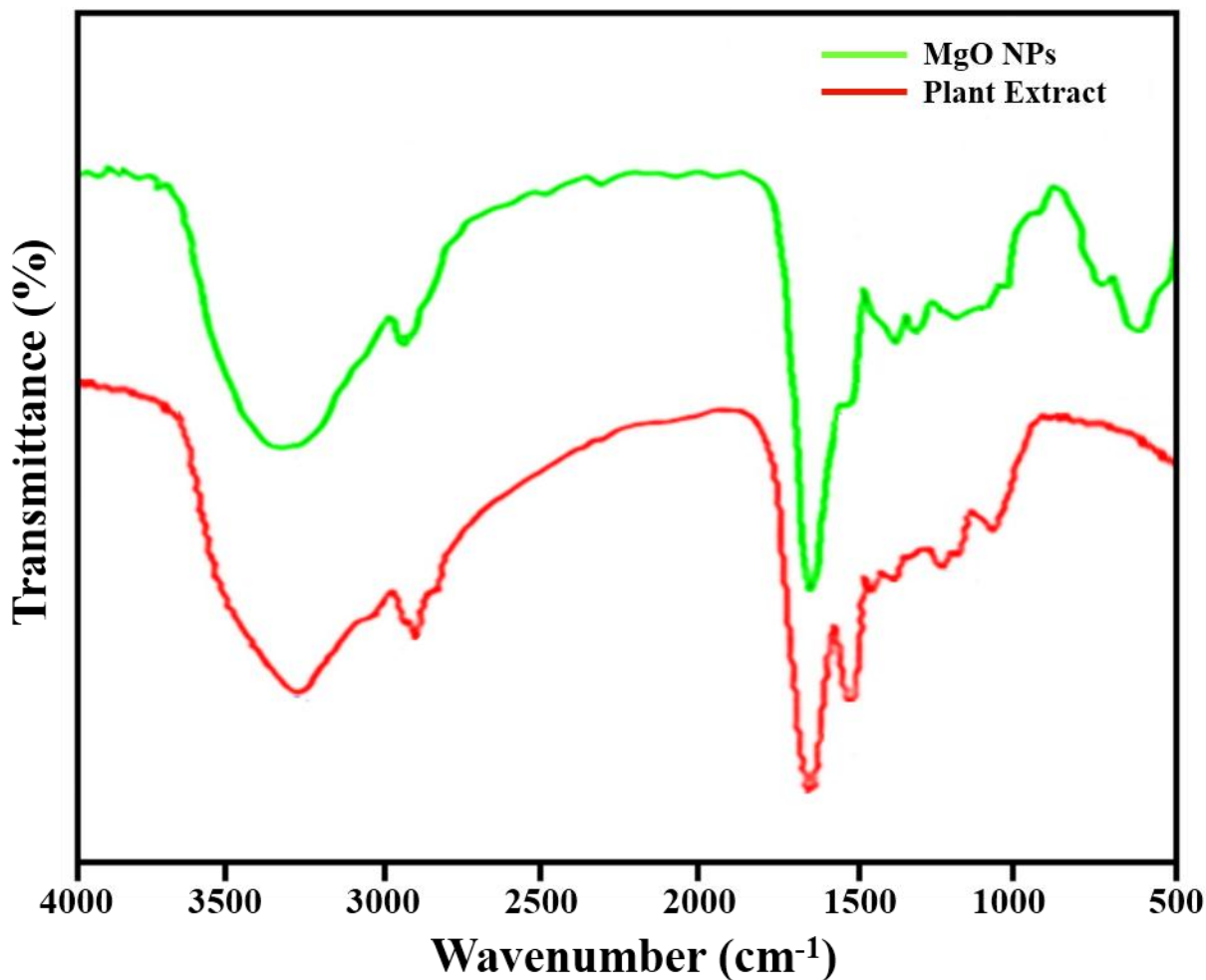


**Figure 3:** FTIR analysis of plant extract and biosynthesized MgO NPs

### 3.3 HRTEM Analysis

HRTEM is an important research technique for the direct imaging of NMs to achieve quantifiable measures of particle size, shape, and dispersion. Figure 4(A) signifies the HRTEM image of plant-mediated magnesium oxide nanoparticles. The microscopic image indicates that MgO nanoparticles are of small size (average size =27 nm), spherical shape with the high distribution. The results are fairly well matched with previously reported work. Due to such features, MgO NPs exhibit outstanding catalytic and biomedical applications.

### 3.4 SEM and EDS analysis

SEM study was accomplished to scrutinize the surface morphology of greener magnesium oxide nanoparticles. The

biogenic nano-scale magnesium oxide particles were perceived in sphere-shaped morphology. The SEM microscopic image of biodirected MgO nanoparticles was taken at a magnification of 800 x, as illustrated in Figure 4(B). The particle size of MgO NPs was observed to be 27 nm. The microscopic image shown that the synthesized MgO NPs aggregated, mostly sphere-shaped and occasional in cubes structures.

EDS study provided qualitative and quantitative analysis of the elements that might be involved in the stabilization and formation of nanoparticles. Figure 4(C) indicates the EDS profile of biogenic magnesium oxide NPs. The peaks in the region of "Mg" and "O" confirm the establishment of MgO nanoparticles.

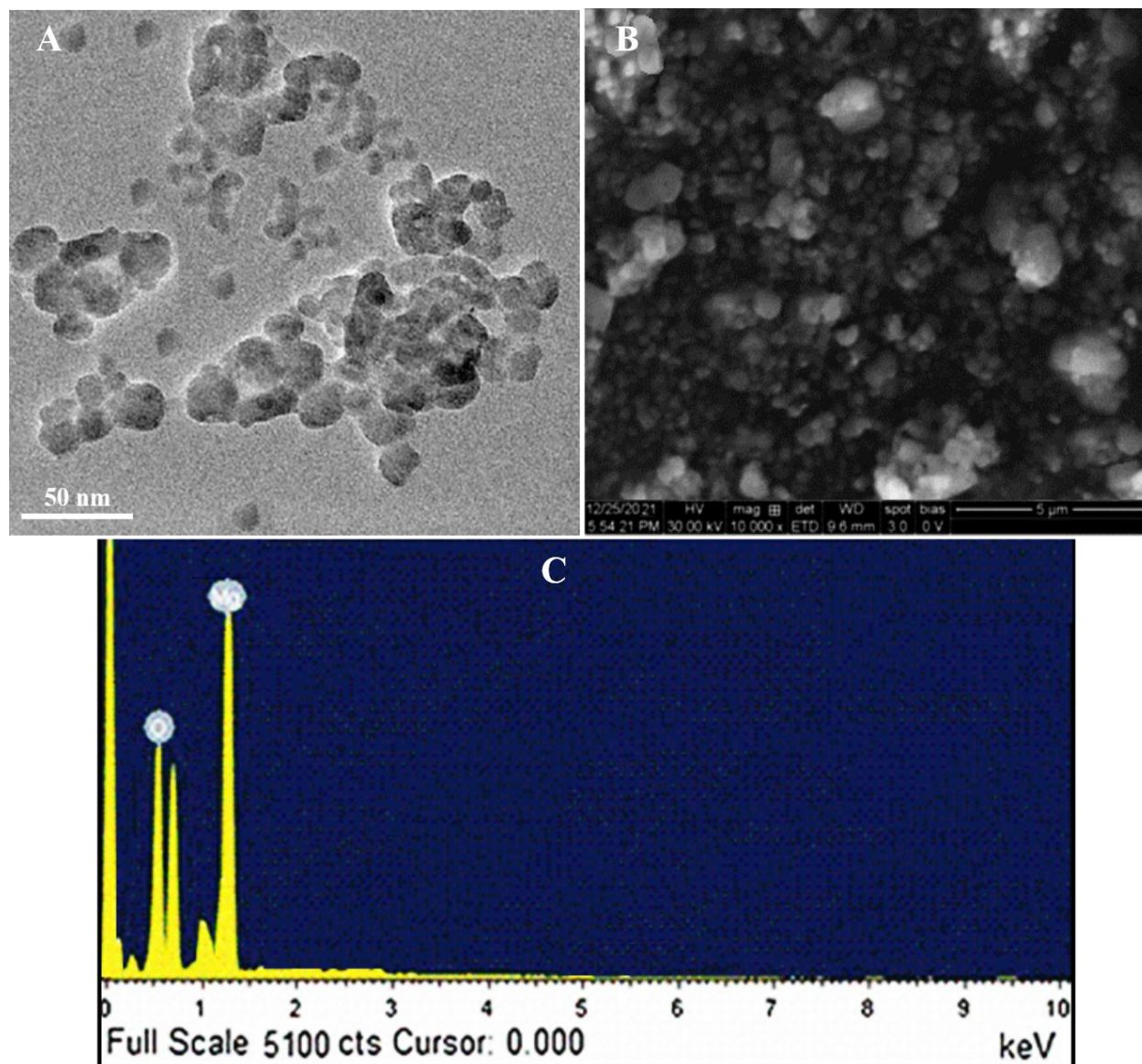


**Figure 5:** (A) HRTEM analysis, (B) SEM analysis, and (C) EDS analysis of Biosynthesized MgO NPs

### 3.5 Antibacterial Activity

Antibacterial activities of plant extract and greener MgO NPs were examined against *S. aureus* and *E. coli* bacteria. The biodirected MgO NPs exhibited higher inhibition efficiency than plant extract against the tested bacteria. The results depicted that MgO NPs significantly apprehend bacterial growth with inhibition zones of  $17(\pm 0.4 \text{ mm})$  and  $16(\pm 0.5 \text{ mm})$  against *S. aureus* and *E. coli* which are more effective than a plant extract of  $11(\pm 0.2 \text{ mm})$  and  $12(\pm 0.4 \text{ mm})$  respectively as given in Table 1. The higher antibacterial action of biodirected MgO NPs may be assigned to

their nano size, spherical shape, and high dispersal. The nanoparticles of smaller size and sphere morphology offer greater surface regions and are consequently highly effective than their bulk particles. This high bacterial inhibition efficiency of the tested NPs can be assigned to producing ROS released by metal oxide ions (47,48). According to literature, control elimination of metal oxides from metal oxide nanoparticles generate superoxide ( $\bullet\text{O}_2^-$ ) and hydroxide ( $\bullet\text{OH}$ ) radicals in harmful microbes (49). When the concentration of these ROS upsurges, then the scavenging ability of bacteria cells will lead to cell death.

**Table 1:** Bacterial Inhibition Efficiency of MgO NPs and Plant Extract against *S.aureus* and *E.coli*

Bacteria	Zones of Inhibition	
	MgO NPs	Plant Extract
<i>S. aureus</i>	17( $\pm$ 0.4 mm)	11( $\pm$ 0.2 mm)
<i>E.coli</i>	16( $\pm$ 0.5 mm)	12( $\pm$ 0.4 mm)

### 3.5.1. MIC Determination

MIC is a useful method for quantitatively evaluating the tested material's antibacterial activity. MIC is the least amount of greener MgO NPs essential to obstruct the growth

of bacteria. A dilute suspension of MgO NPs was incubated with *S. aureus*, and *E. coli* strains at 37 °C for 24 hrs in a shaking incubator. As shown in Table 2, after incubation, it was discovered that *S. aureus* and *E. coli* showed MICs of 0.125 mg/mL.

**Table 2:** MIC of MgO NPs against *S. aureus* and *E. coli*.

Bacteria	MgO NPs(mg/mL)			
	1	0.5	0.25	0.125
<i>S. aureus</i>	-	-	-	+
<i>E.coli</i>	-	-	-	+

## 4. Conclusion

Among other conservative protocols to synthesize nano-scale materials, biogenic routes are a promising field that offers an innocuous, biodegradable, and valuable procedure to manufacture innovative materials. In this work, we present a biogenic production of magnesium oxide NPs using leaf extract of *C. erectus*. The phyto constituents of plant extract performed a prominent role in the formation and stabilization magnesium oxide NPs. The size and shape of MgO NPs were optimized at 70 °C. The greener MgO nanoparticles were inspected for bacterial inhibition activity against *S. aureus* and *E. coli*. Thus, MgO NPs have actively reserved the *S. aureus* and *E. coli* growth with zones of inhibition of 17( $\pm$ 0.4) mm and 16( $\pm$ 0.5) mm, respectively. This high efficiency of greener MgO NPs can be attributed to their nano size and a high degree of dispersion. The as-synthesized MgO NPs may necessitate further investigation and additional applications.

**Acknowledgement** We thank the Beijing University of Chemical Technology (BUCT) for the characterization of our samples. All the authors have approved the manuscript.

**Conflict of Interest** There is no conflict of interest

## References

1. Laurent S, Forge D, Port M, Roch A, Robic C, Vander Elst L, Muller RN. Magnetic iron oxide nanoparticles: synthesis, stabilization, vectorization, physicochemical characterizations, and biological applications. *Chemical reviews*. 2008 Jun 11;108(6):2064-110.
2. Wojcieszak R, Genet MJ, Eloy P, Gaigneaux EM, Ruiz P. Supported Pd nanoparticles prepared by a modified water-in-oil microemulsion method. *In Studies in Surface Science and Catalysis 2010 Jan 1 (Vol. 175, pp. 789-792)*. Elsevier.
3. Rao KG, Ashok CH, Rao KV, Chakra CS. Structural properties of MgO nanoparticles: synthesized by co-precipitation technique.

- International Journal of Science and Research. 2014;3(12):43-6.
4. El-Argawy E, Rahhal MM, El-Korany A, Elshabrawy EM, Eltahan RM. Efficacy of some nanoparticles to control damping-off and root rot of sugar beet in El-Behiera Governorate. *Asian J Plant Pathol.* 2017;11:35-47.
  5. Zhong L, Liu H, Samal M, Yun K. Synthesis of ZnO nanoparticles-decorated spindle-shaped graphene oxide for application in synergistic antibacterial activity. *Journal of Photochemistry and Photobiology B: Biology.* 2018 Jun 1;183:293-301.
  6. Abdallah Y, Ogunyemi SO, Abdelazez A, Zhang M, Hong X, Ibrahim E, Hossain A, Fouad H, Li B, Chen J. The green synthesis of MgO nano-flowers using *Rosmarinus officinalis L.* (Rosemary) and the antibacterial activities against *Xanthomonas oryzae*. *BioMed Research International.* 2019 Oct;2019.
  7. Salehifar N, Zarghami Z, Ramezani M. A facile, novel and low-temperature synthesis of MgO nanorods via thermal decomposition using new starting reagent and its photocatalytic activity evaluation. *Materials Letters.* 2016 Mar 15;167:226-9.
  8. Suresh J, Pradheesh G, Alexramani V, Sundrarajan M, Hong SI. Green synthesis and characterization of hexagonal shaped MgO nanoparticles using insulin plant (*Costus pictus D. Don*) leave extract and its antimicrobial as well as anticancer activity. *Advanced Powder Technology.* 2018 Jul 1;29(7):1685-94.
  9. Roselli M, Finamore A, Garaguso I, Britti MS, Mengheri E. Zinc oxide protects cultured enterocytes from the damage induced by *Escherichia coli*. *The Journal of nutrition.* 2003 Dec 1;133(12):4077-82.
  10. Sawai J. Quantitative evaluation of antibacterial activities of metallic oxide powders (ZnO, MgO and CaO) by conductimetric assay. *Journal of microbiological methods.* 2003 Aug 1;54(2):177-82.
  11. Sawai J, Kojima H, Igarashi H, Hashimoto A, Shoji S, Sawaki T, Hakoda A, Kawada E, Kokugan T, Shimizu M. Antibacterial characteristics of magnesium oxide powder. *World Journal of Microbiology and Biotechnology.* 2000 Mar;16(2):187-94.
  12. Ali J, Irshad R, Li B, Tahir K, Ahmad A, Shakeel M, Khan NU, Khan ZU. Synthesis and characterization of phytochemical fabricated zinc oxide nanoparticles with enhanced antibacterial and catalytic applications. *Journal of Photochemistry and Photobiology B: Biology.* 2018 Jun 1;183:349-56.
  13. Tahir K, Ahmad A, Li B, Nazir S, Khan AU, Nasir T, Khan ZU, Naz R, Raza M. Visible light photocatalytic inactivation of bacteria and photo degradation of methylene blue with Ag/TiO<sub>2</sub> nanocomposite prepared by a novel method. *Journal of Photochemistry and Photobiology B: Biology.* 2016 Sep 1;162:189-98.
  14. Elegbede JA, Lateef A, Azeez MA, Asafa TB, Yekeen TA, Oladipo IC, Adebayo EA, Beukes LS, Gueguim-Kana EB. Fungal xylanases-mediated synthesis of silver nanoparticles for catalytic and biomedical applications. *IET nanobiotechnology.* 2018 Sep;12(6):857-63.
  15. Fouad H, Hongjie L, Yanmei D, Baoting Y, El-Shakh A, Abbas G, Jianchu M. Synthesis and characterization of silver nanoparticles using *Bacillus amyloliquefaciens* and *Bacillus subtilis* to control filarial vector *Culex pipiens pallens* and its antimicrobial activity. *Artificial Cells, Nanomedicine, and Biotechnology.* 2017 Oct 3;45(7):1369-78.
  16. Ogunyemi SO, Abdallah Y, Zhang M, Fouad H, Hong X, Ibrahim E, Masum MM, Hossain A, Mo J, Li B. Green synthesis of zinc oxide nanoparticles using different plant extracts and their antibacterial activity against *Xanthomonas oryzae*. *Artificial cells, nanomedicine, and biotechnology.* 2019 Dec 4;47(1):341-52.
  17. Saravanakumar K, Chelliah R, Shanmugam S, Varukattu NB, Oh DH, Kathiresan K, Wang MH. Green synthesis and characterization of biologically active nanosilver from seed extract of *Gardenia jasminoides Ellis*. *Journal of Photochemistry and Photobiology B: Biology.* 2018 Aug 1;185:126-35.
  18. Ogunyemi SO, Zhang F, Abdallah Y, Zhang M, Wang Y, Sun G, Qiu W, Li B. Biosynthesis and characterization of magnesium oxide and manganese dioxide nanoparticles using *Matricaria chamomilla L.* extract and its inhibitory effect on *Acidovorax oryzae* strain RS-2. *Artificial cells, nanomedicine, and biotechnology.* 2019 Dec 4;47(1):2230-9.



19. Wypij M, Czarnecka J, Świecimska M, Dahm H, Rai M, Golinska P. Synthesis, characterization and evaluation of antimicrobial and cytotoxic activities of biogenic silver nanoparticles synthesized from *Streptomyces xinghaiensis* OF1 strain. *World Journal of Microbiology and Biotechnology*. 2018 Feb;34(2):1-3.
20. Mohanraj R. Antimicrobial activities of metallic and metal oxide nanoparticles from plant extracts. In *Antimicrobial Nanoarchitectonics 2017* Jan 1 (pp. 83-100). Elsevier.
21. Yuvakkumar R, Hong SI. Green synthesis of spinel magnetite iron oxide nanoparticles. In *Advanced Materials Research 2014* (Vol. 1051, pp. 39-42). Trans Tech Publications Ltd.
22. Kumar B, Smita K, Cumbal L, Debut A, Camacho J, Hernández-Gallegos E, de Guadalupe Chávez-López M, Grijalva M, Angulo Y, Rosero G. Pomo-synthesis and biological activity of silver nanoparticles using *Passifloratripartita* fruit extracts. *Advanced Materials Letters*. 2015 Feb 1;6(2):127-32.
23. Vergheese M, Vishal SK. Green synthesis of magnesium oxide nanoparticles using *Trigonellafoenum-graecum* leaf extract and its antibacterial activity. *J PharmacognPhytochem*. 2018;7(3):1193-200.
24. Kumar B, Smita K, Cumbal L, Debut A, Camacho J, Hernández-Gallegos E, de Guadalupe Chávez-López M, Grijalva M, Angulo Y, Rosero G. Pomo-synthesis and biological activity of silver nanoparticles using *Passifloratripartita* fruit extracts. *Advanced Materials Letters*. 2015 Feb 1;6(2):127-32.
25. Jhansi K, Jayarambabu N, Reddy KP, Reddy NM, Suvarna RP, Rao KV, Kumar VR, Rajendar V. Biosynthesis of MgO nanoparticles using mushroom extract: effect on peanut (*Arachis hypogaea* L.) seed germination. *3 Biotech*. 2017 Aug;7(4):1-1.
26. Abdallah Y, Ogunyemi SO, Abdelazez A, Zhang M, Hong X, Ibrahim E, Hossain A, Fouad H, Li B, Chen J. The green synthesis of MgO nano-flowers using *Rosmarinus officinalis* L. (Rosemary) and the antibacterial activities against *Xanthomonas oryzae* pv. *oryzae*. *BioMed Research International*. 2019 Oct;2019.
27. Vergheese M, Vishal SK. Green synthesis of magnesium oxide nanoparticles using *Trigonellafoenum-graecum* leaf extract and its antibacterial activity. *J PharmacognPhytochem*. 2018;7(3):1193-200.
28. Ramanujam K, Sundrarajan M. Antibacterial effects of biosynthesized MgO nanoparticles using ethanolic fruit extract of *Embllica officinalis*. *Journal of photochemistry and photobiology B: biology*. 2014 Dec 1;141:296-300.
29. Vergheese M, Vishal SK. Green synthesis of magnesium oxide nanoparticles using *Trigonellafoenum-graecum* leaf extract and its antibacterial activity. *J PharmacognPhytochem*. 2018;7(3):1193-200.
30. Ogunyemi SO, Zhang F, Abdallah Y, Zhang M, Wang Y, Sun G, Qiu W, Li B. Biosynthesis and characterization of magnesium oxide and manganese dioxide nanoparticles using *Matricaria chamomilla* L. extract and its inhibitory effect on *Acidovorax oryzae* strain RS-2. *Artificial cells, nanomedicine, and biotechnology*. 2019 Dec 4;47(1):2230-9.
31. Weakley AS. Flora of the southern and mid-Atlantic states.
32. Abdel-Hameed ES, Bazaid SA, Shohayeb MM, El-Sayed MM, El-Wakil EA. Phytochemical studies and evaluation of antioxidant, anticancer and antimicrobial properties of *Conocarpus erectus* L. growing in Taif, Saudi Arabia. *European Journal of Medicinal Plants*. 2012 Apr 1;2(2):93.
33. Al-Wabel MI, Usman AR, El-Naggar AH, Aly AA, Ibrahim HM, Elmaghraby S, Al-Omran A. *Conocarpus* biochar as a soil amendment for reducing heavy metal availability and uptake by maize plants. *Saudi journal of biological sciences*. 2015 Jul 1;22(4):503-11.
34. Nascimento DK, Souza IA, Oliveira AF, Barbosa MO, Santana MA, Pereira Junior DF, Lira EC, Vieira JR. Phytochemical screening and acute toxicity of aqueous extract of leaves of *Conocarpus erectus* Linnaeus in swiss albino mice. *Anais da Academia Brasileira de Ciências*. 2016 Aug 4;88:1431-7.
35. Raza MA, Anwar F, Shahwar D, Majeed A, Mumtaz MW, Danish M, Nazar MF, Perveen I, Khan SU. Antioxidant and antiacetylcholine esterase potential of aerial parts of *Conocarpus erectus*, *Ficus variegata* and *Ficus maclellandii*. *Pakistan journal of pharmaceutical sciences*. 2016 Mar 1;29(2).

36. Raza SA, Chaudhary AR, Mumtaz MW, Ghaffar A, Adnan A, Waheed A. Antihyperglycemic effect of *Conocarpus erectus* leaf extract in alloxan-induced diabetic mice. *Pakistan journal of pharmaceutical sciences*. 2018 Mar 2;31.
37. Santos DK, de Almeida VS, de Araujo DR, Harand W, Soares AK, Moreira LR, de Lorena VM, Magalhães LP, Ximenes RM, de Sena KX, de Melo CM. Evaluation of cytotoxic, immunomodulatory and antibacterial activities of aqueous extract from leaves of *Conocarpus erectus* Linnaeus (Combretaceae). *Journal of Pharmacy and Pharmacology*. 2018 Aug;70(8):1092-101.
38. Abdel-Hameed ES, Bazaid SA, Sabra AN. Protective effect of *conocarpus erectus* extracts on CCl<sub>4</sub>-induced chronic liver injury in mice. *Glob J Pharmacol*. 2013;7(1):52-60.
39. Hussein RA. Evaluation antioxidant and antibacterial activities of n-Butanol fraction of *Conocarpus erectus* L. leaves extract. *Int J Pharm Med Res*. 2016 Dec 25;4(6):394-400.
40. Bashir M, Uzair M, Chaudhry BA. A review of phytochemical and biological studies on *Conocarpus erectus* (Combretaceae). *Pak J Pharm Res*. 2015;1(1):1-8.
41. Rehman S, Azam F, Rehman S, Rehman TU, Mehmood A, Gohar A, Samad A. A review on botanical, phytochemical and pharmacological reports of *conocarpus erectus*. *Pak J Agric Res*. 2019;32(1):212-7.
42. Ayoub NA. A trimethoxyellagic acid glucuronide from *Conocarpus erectus* leaves: Isolation, characterization and assay of antioxidant capacity. *Pharmaceutical biology*. 2010 Mar 1;48(3):328-32.
43. Nascimento DK, Souza IA, Oliveira AF, Barbosa MO, Santana MA, Pereira Junior DF, Lira EC, Vieira JR. Phytochemical screening and acute toxicity of aqueous extract of leaves of *Conocarpus erectus* Linnaeus in swiss albino mice. *Anais da Academia Brasileira de Ciências*. 2016 Aug 4;88:1431-7.
44. Khan SA, Shahid S, Ijaz F. Green Synthesis of Copper oxide Nanoparticles & Biomedical Application. LAP LAMBERT Academic Publishing; 2017.
45. Ghosh R, Kundu S, Majumder R, Roy S, Das S, Banerjee A, Guria U, Banerjee M, Bera MK, Subhedar KM, Chowdhury MP. One-pot synthesis of multifunctional ZnO nanomaterials: study of superhydrophobicity and UV photosensing property. *Applied Nanoscience*. 2019 Nov;9(8):1939-52.
46. Nordin NR, Shamsuddin M. Biosynthesis of copper (II) oxide nanoparticles using *Murayyakoeniggi* aqueous leaf extract and its catalytic activity in 4-nitrophenol reduction. *Malaysian Journal of Fundamental and Applied Sciences*. 2019;15:218-24.
47. Li Y, Zhang W, Niu J, Chen Y. Surface-coating-dependent dissolution, aggregation, and reactive oxygen species (ROS) generation of silver nanoparticles under different irradiation conditions. *Environmental science & technology*. 2013 Sep 17;47(18):10293-301.
48. Li Y, Zhang W, Niu J, Chen Y. Mechanism of photogenerated reactive oxygen species and correlation with the antibacterial properties of engineered metal-oxide nanoparticles. *ACS nano*. 2012 Jun 26;6(6):5164-73.
49. Tahir K, Nazir S, Ahmad A, Li B, Khan AU, Khan ZU, Khan FU, Khan QU, Khan A, Rahman AU. Facile and green synthesis of phytochemicals capped platinum nanoparticles and in vitro their superior antibacterial activity. *Journal of Photochemistry and Photobiology B: Biology*. 2017 Jan 1;166:246-51.